ISSN 1738-3935
New & Renewable Energy 2012. 9 Vol. 8, No. 3 http://dx.doi.org/10.7849/ksnre.2012.8.3.006

논문 1

[2012-09-FC-001]

연료전지용 캐소드 공기블로어의 비정상 내부유동장 연구

장춘만*, 이종성

Unsteady Internal Flow Analysis of a Cathode Air Blower Used for Fuel Cell System

Choonman Jang* and Jongsung Lee

Abstract This paper describes unsteady internal flow characteristics of a cathode air blower, used for the 1 kW fuel cell system. The cathode air blower considered in the present study is a diaphragm type blower. To analyze the flow field inside the diaphragm cavity, compressible unsteady numerical simulation is performed. Moving mesh system is applied to the numerical analysis for describing the volume change of the diaphragm cavity in time. Throughout a numerical simulation by modeling the inlet and outlet valves in a diaphragm cavity, unsteady nature of an internal flow is successfully analyzed. Variations of mass flow rate, force and pressure on the lower moving plate of a diaphragm cavity are evaluated in time. The computed mass flow rate at the same pressure and rotating frequency of a motor has a maximum of 5 percent error with the experimental data. It is found that flow pattern at the suction process is more complex compared to that at the discharge process. Unsteady nature of internal flow in the cathode air blower is analyzed in detail.

Key words Fuel cell system(연료전지 시스템), Unsteady analysis(비정상 해석), Cathode air blower(캐소드 공기블로어), Pressure(압력), Diaphragm cavity(다이어프램 캐비티)

(접수일 2012. 6. 19, 수정일 2012. 8. 9, 게재확정일 2012. 8. 9)

* 한국건설기술연구원 (Environmental Engineering Research Division, Korea Institute of Construction Technology)
■ E-mail : jangcm@kict.re.kr ■ Tel : (031)910-0494 ■ Fax : (031)910-0291

1. Introduction

The 1 kW fuel cell system has been developed to apply for the green home project, started from 2008 as new growth power industries supported by Korean government. Among the BOP of a 1 kW fuel cell system, manufacturing process with low price and high efficiency is important in the view point of the market share and operating energy reduction of the system. Air blower of a fuel cell system can be divided into two structures: one is diaphragm type and the other is rotating type. In a small system like a 1 kW fuel cell system, diaphragm type is mainly selected by manufacturing cost and its compactness. It is reported that the cost of BOP reaches to 47 % among the total system on the base of 10,000 productions per year[1].

Until today, a lot of works have been carried out to

improve the efficiency of various blowers such as centrifugal type[2,3], axial type[4] and regenerative type[5,6] etc. and to find optimal shape and operating conditions as well. They have given a many concept of significant design factors for the various blowers, and these conceptualized factors have been translated into mathematical forms by fan theory.

However only a few works has been done for the evaluation of efficiency and characteristics of performance on a diaphragm type blower(Jang et al.[7,8] studied the internal flow of a fuel pressurized blower by numerical simulation and experimental measurement. They represents some of the optimal shape of a fuel cell blower using the modeled shape of a diaphragm cavity). In order to improve the performance of the diaphragm type blower, characteristics of internal flow fields for the fundamental work, should be clarified. And then, design optimization for the various shapes and control variables will be performed as a global optimization method like a response surface method[9,10].

The objectives of a present work is to clarify the unsteady internal flow of a diaphragm type blower and to find a important factors influencing the blower performance by experimental measurements and three-dimensional unsteady numerical simulation.

2. Test Blower

In the fuel cell system, generally three types of an air blower and one gas blower are installed as shown in Fig. 1. A cathode air blower installed in a fuel cell system is introduced in the present study. As shown in Fig. 2, the blower system mainly consists of two diaphragms, a driving motor, valves and inlet/ outlet ports. In the diaphragm as shown in Fig. 2(b), there are stationary and moving parts. In the figure, a moving plate located at the lower part of the diaphragm cavity is oscillating with sinusoidal curve by a cam connected to a driving motor.

Table 1 shows the specifications of a test blower at the normal operating condition. Flow rate and pressure are 55.2 lpm and 12 kPa, respectively. Rotational frequency of a driving motor is 2,200 rpm, which corresponds to 0.02727 sec for one cycle. Vertical movement of a moving plate is shown in Fig. 3. Maximum vertical displacement of a moving plate is 5 mm.

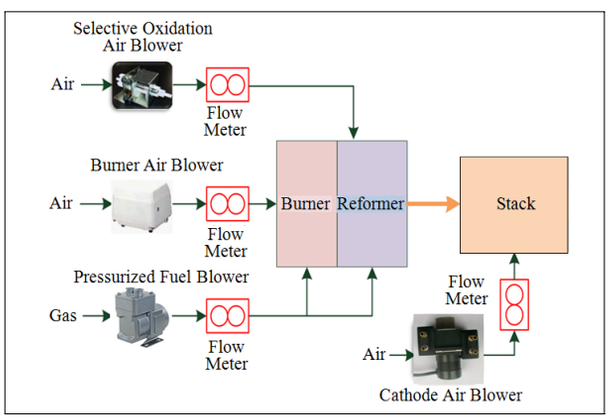

Fig. 1 Layout of fuel cell system and blowers

Table 1. Specifications of a test blower at the operating condition

Name	value
Pressure, kPa	12
Rotational frequency of a Motor, rpm	2,200
Flow rate, lpm	55.2

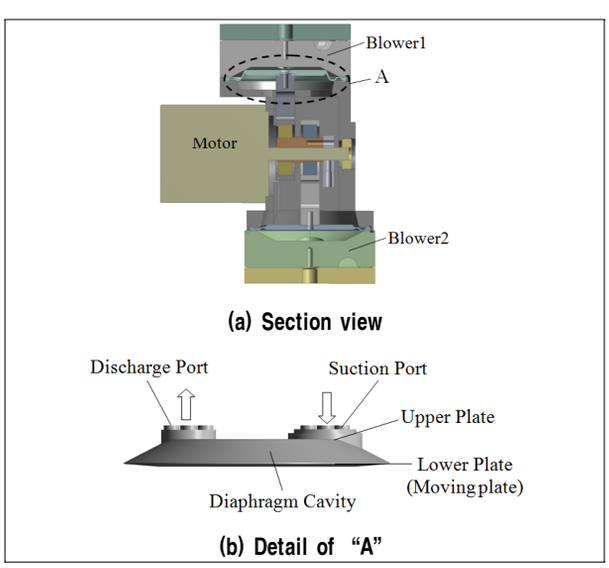

Fig. 2 Test cathode air blower

Figure 4 shows the schematic view of the experimental set-up, which is an open-loop facility. The facility mainly consists of a flow control valve, a damper, a mass flow controller, sensors and a compressor. Flow rate is determined at the downstream of a damper.

The control system of flow and pressure with proportional control method is installed for the varying of RPM and flow rates and for the keeping of constant measuring conditions. Therefore performance curve of the test blower could be obtained as shown in Fig. 5.

At the normal operating condition of 2,200 rpm, the measuring flow rate is 55.2 lpm while the pressure is 12 kPa and its efficiency is 43.1%.

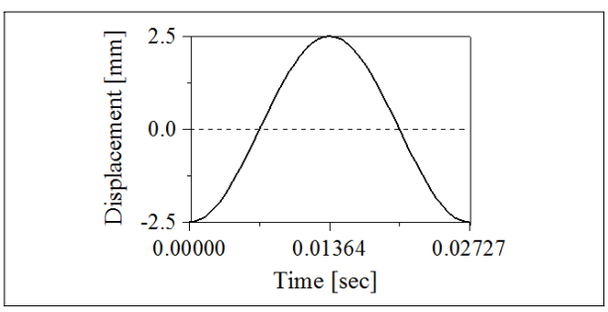

Fig. 3 Vertical displacement of a moving plate for one cycle

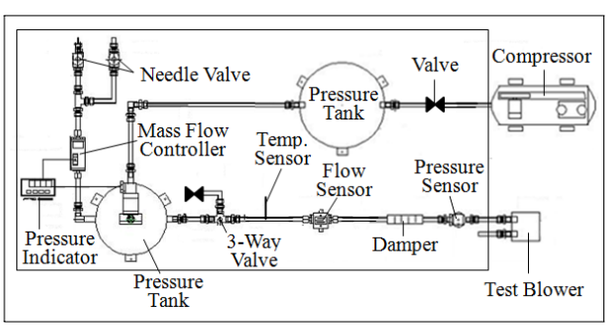

Fig. 4 Layout of experimental apparatus

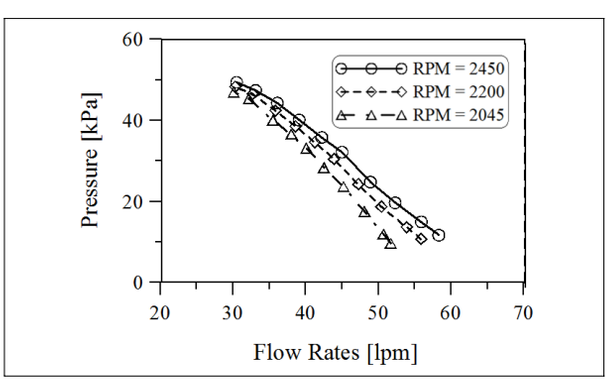

Fig. 5 Performance curve of test cathode air blower

3. Numerical Simulation and Boundary Conditions

3.1 Numerical simulation method

To analyze three-dimensional flow field in a cathode air blower, general commercial code, CFX-13[11], is employed in the present work. It solves compressible unsteady Reynolds-averaged Navier-Stokes equations and continuity equation. SST k-ω turbulence model with scalable wall function is employed to more accurate estimate adverse pressure gradient flows[12].

For the modeling of the vertical movement of the moving plate due to the eccentricity of a cam, moving mesh system is introduced. Considering the one cyclic movement of the moving plate, time interval is divided by 60 times per one cycle.

In computational grids, unstructured grids are used to represent a composite grid system including the diaphragm cavity. Figure 6 shows the computational grid system. Tetrahedral element is imposed in the diaphragm cavity where wedge (prism) element having two layers is given near the inlet and outlet ports. The whole grid system in the present simulation for a test fan has 296,629 nodes (1,337,603 elements). Side view of full suction and discharge conditions is shown in Figs. 6(b) and 6(c), respectively.

Table 2. Validation of the operating condition

Name	Exp.	CFD	Error
Pressure, kPa	12	12	–
Rotational frequency of a motor, rpm	2,200	2,200	
Flow rate, lpm	55.2	58.1	5 %

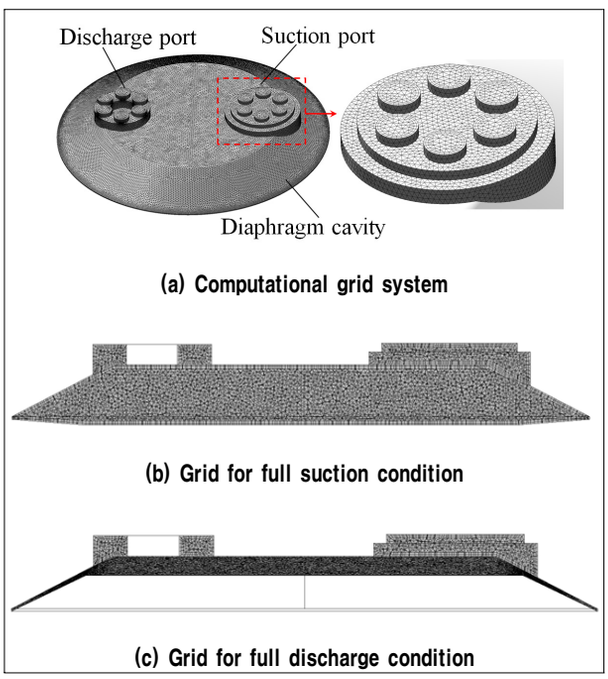

Fig. 6 Computational grids

3.2 Boundary condition

Relative pressure of 0 Pa is specified at the inlet, and relative pressure of 12 kPa is specified at the outlet plane. The pressure at the outlet is determined by considering design operation condition. The outlet valve is opened at the condition above the pressure of 12 kPa for the discharge process. No-slip and adiabatic wall conditions are used on wall and duct surfaces.

4. Results and Discussion

4.1 Comparisons of experimental and numerical results

For the validation of the present numerical solutions, mass flow rate obtained at the design operation condition is compared with the experimental result as shown in Table 2. The computed mass flow rate at the same pressure and rotating frequency of a motor has a maximum of 5 percent error with the experimental data. The comparison between the numerical and experimental results shows that the mass flow rate of the test blower is simulated correctly by the present calculation.

4.2 Unsteady nature of internal flow

Figure 7 shows the variations of mass flow at the outlet and inlet planes in time. The calculation time of the internal flow for the blower is 0.08181sec, which corresponds to three cycle of the moving plate. As shown in Fig. 7, the results of numerical simulation for the first one cycle are unstable, because the flow field is not developed enough from start simulation. Therefore, numerical results after two cycles could be analyzed.

Variation of mass flow rate in time are represented by the dashed and solid lines, respectively. In the discharge process for the second cycle, valve installed at outlet duct is closed for the compression time of 1/6 cycle ("dt" in Fig.7). After then, compressed air moves out through outlet duct. The total flow rate through outlet duct is 58.1 lpm while the pressure at the outlet keeps 12 kPa. After finishing the discharge process, suction valve is opened. Therefore, it is known that total flow rate calculated for the discharge and suction process has a same value of 58.1 lpm and well simulated.

Figure 8 shows the variations of pressure on the center of the moving plate in time. Measuring position of pressure is shown in Fig. 8(a), which is the top view of the diaphragm cavity. Pressure on the moving plate is increased rapidly while the discharge process is progressed for "dt" time. In the period of "dt", the valve at the outlet duct is closed condition. In the discharge process after the valve at the outlet duct is opened, pressure at the outlet plane keeps almost same value of 12 kPa. It is no use to say that pressure goes to atmospheric condition while suction process as shown in Fig. 7.

Figure 9 shows the variations of normal force on the

moving plate in time. Normal force on the moving plate corresponds to the motor driving force directly. The force on the moving plate is rapidly increased while the discharge process is progressed for "dt" time. The local force on the moving plate is about 25.4 N.

Generally, limiting streamlines is very effective method to understand internal flow structure because they represent shear flow direction on the surface. Limiting streamlines

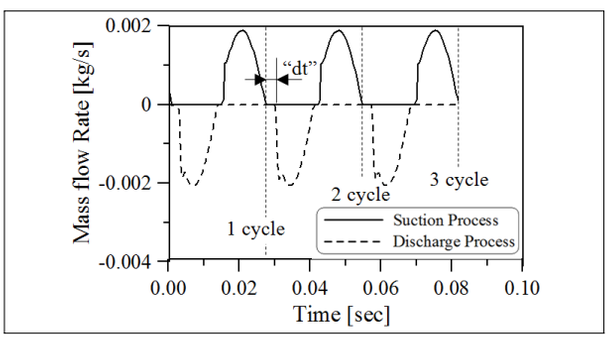

Fig. 7 Variations of mass flow rate in time

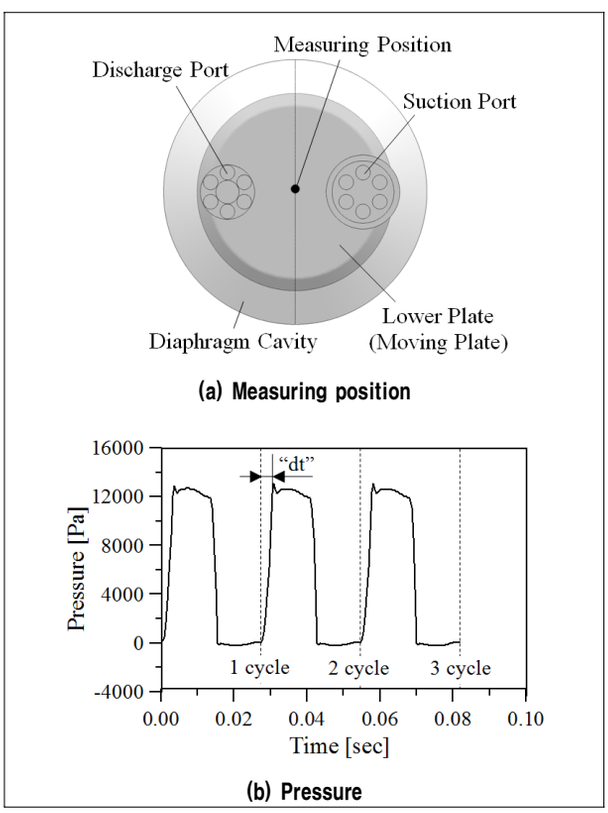

Fig. 8 Pressure on the lower moving plate in time

on the moving plate in time are analyzed as shown Fig. 10. The left figure represents the positions of a moving plate with the section view of a diaphragm cavity. As described in Fig. 3, the moving plate is located at the bottom of a diaphragm cavity when time is zero. The view point of the right figure is same in Fig. 8(a).

From the limiting streamline on the moving plate at time zero, flow is separated to the suction and discharge sides with a separation line. Large circulation flow is observed in the discharge side (left side in the figure). Second figure shows the limiting streamlines at the middle of discharge process. Due to the outflow through outlet duct, flow towards to the discharge side from suction side.

The third figure shows the streamlines at the end of discharge process. At this time, flow moves from discharge side to suction side at the bottom of the cavity. The last figure in Fig. 10 shows limiting streamlines at the middle of suction process. At this time, it can be found the separated flow between the discharge and suction sides. This flow pattern is similar to that in the limiting streamlines at time zero. Then, same cycle is continually repeated.

From the Fig. 10, it could be clearly understood the different flow pattern during between discharge and suction processes. At the suction process, flow has a no directivity.

That's why, suction process is more complex compared to that the discharge process. In suction process, high

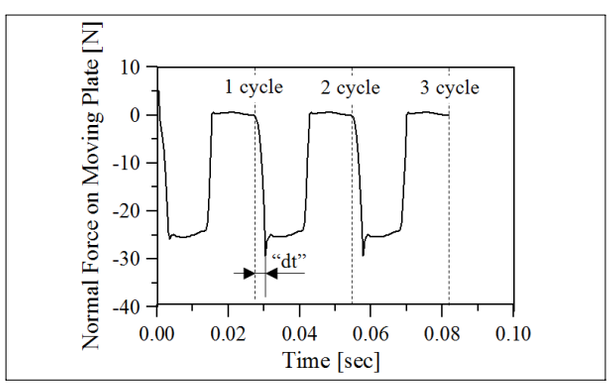

Fig. 9 Variations of normal force on the moving plate in time

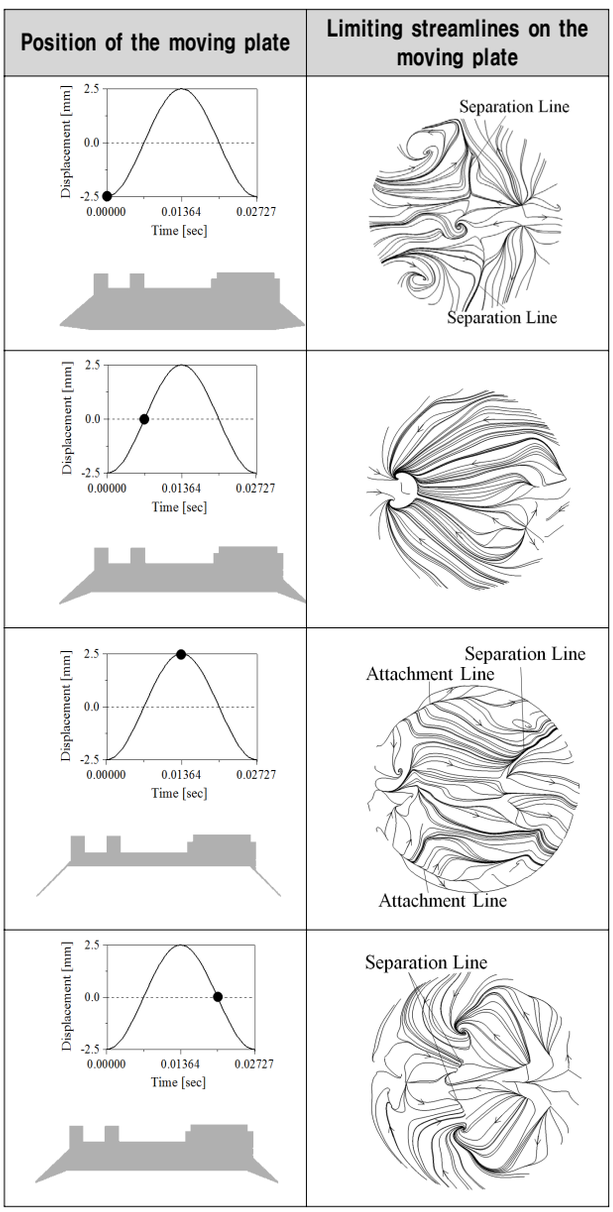

Fig. 10 Limiting streamlines on the moving plate in time

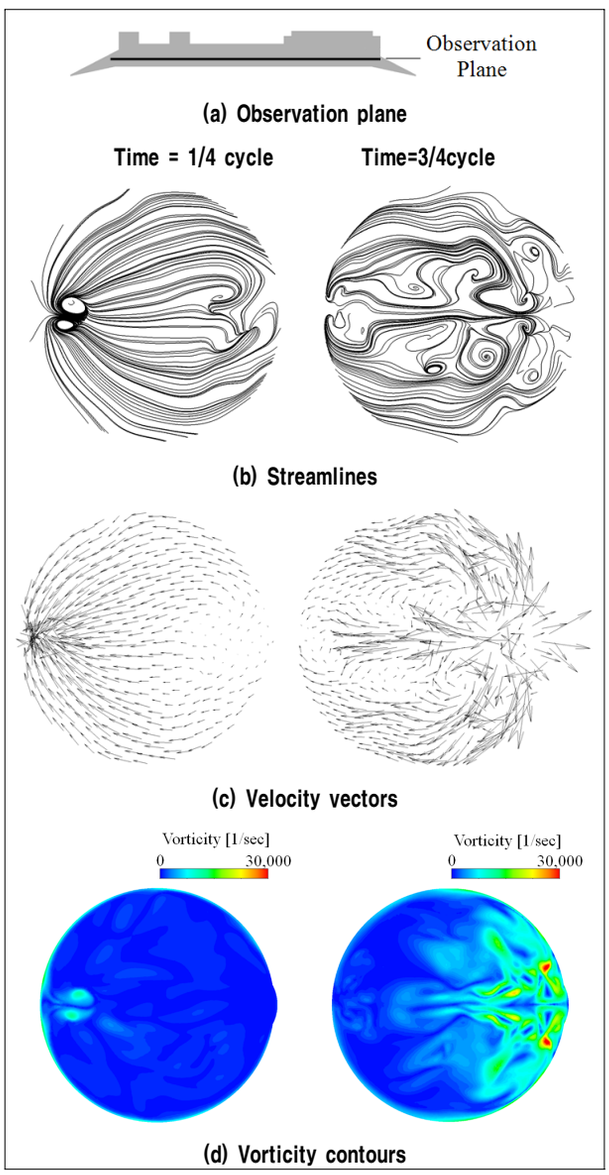

Fig. 11 Projected streamlines, velocity vectors and vorticity on the mid-plane at the time of 1/4 and 3/4 cycle

unsteady flow with the interaction between separation and attachment lines is observed, thus deteriorates blower efficiency.

Figure 11 shows the projected streamlines, velocity vectors and vorticity on the mid-plane at the time of 1/4 and 3/4 cycle, which are at the moment of mid suction and discharge process. The observation plane is shows in Fig. 11(a), which is on the middle plane of the diaphragm cavity. From the projected streamline on the plane in Fig. 11(b), very complex swirl flows are generated by the inflow of the air when start suction process. And, it also could be known that velocity and vorticity gradient have very high value in Fig. 11(c) and (d).

These vortical flows direct connect to pressure loss factors and unsteadiness. This means that discharge process is more stable than opposite process.

5. Conclusion

The present study describes the unsteady internal flow of a cathode air blower used for a 1kW fuel cell system. Performance measurements are made using an open-loop system over the range of RPM from 2045 to 2450 with various flow rates. Unsteady compressible RANS equations have been applied to a diaphragm cavity during discharge and suction processes. For the modeling of the vertical moving plate in the diaphragm cavity, moving mesh system is introduced. The results of the experimental measurements have a good agreement with the results of the numerical simulation.

The results shows that the force on the moving plate of a diaphragm cavity is rapidly increased while the discharge process is progressed with closed condition of the outlet valve.

It is noted that high unsteady flow with the interaction between separation and attachment lines is observed in the suction process, thus deteriorates blower efficiency. On the other hand, relatively small vortical and swirl flow is observed at discharge process, which means that discharge process is more stable than opposite process.

Acknowledgement

This research was supported by the Korea Institute of Energy Technology Evaluation and Planning (KETEP) grant funded by the Ministry of Knowledge Economy.

References

[1] CFX-13 User Manual, 2010, Ansys Inc.

[2] Choi, K. R. and Jang, C. M., 2011, "Internal Flow Analysis of a Fuel Pressurized Blower for Fuel Cell System", J. of KSNRE, Vol. 9, No. 3, pp. 29-35.

[3] Chon, Y., Kim, K. I. and Kim, K., 1993, "A Knowledgebased System for Centrifugal Fan Blade", Journal of Engineering Applications of Artificial Intelligence, Vol. 6, No. 5, pp. 425-435.

[4] Jang, C. M. and Lim, S. J., 2011, "Performance Analysis of Diaphragm Blower for Fuel Cell", Proceeding of 2010 SAREK Conference, pp. 1006-1011.

[5] Jang, C. M., and Han, G. Y., 2010, "Enhancement of Performance by Blade Optimization in Two-Stage Ring Blower", J. of Thermal Science, Vol. 19, No. 5, pp. 383-389.

[6] Jang, C. M., Choi, S. M., and Kim, K. Y., 2006, "Performance Characteristics of an Axial Flow Fan According to the Shape of a Hub Cap", Journal of Fluid Machinery, Vol. 9, No. 6, pp. 9-16.

[7] Kim, Y. H., and Kang, S. H., 2006, "Performance Evaluation of a Regenerative Blower for Hydrogen Recirculation Application in Fuel Cell Vehicles", Proceedings of ASME Joint U.S. European Fluids Engineering Summer Meeting, FEDSM 2006-98502.

[8] Menter, F. R., 1994, "Two-Equation Eddy-Viscosity Turbulence Models for Engineering Applications", AIAA Journal, Vol. 32, No. 8, pp. 1598-1605.

[9] Myers, R. H., and Montgomery, D. C., 1995, "Response Surface Methodology: Process and Product Optimization Using Designed Experiments", John Wiley & Sons, New york.

[10] N. N. Bayomi, N. Abdel Hafiz and A. M. Osman, 2006, "Effect of Inlet Straighteners on Centrifugal Fan Performance", Energy Conversion & Management, Vol. 47, pp. 3307-3318.

[11] Nagata, 2006, "Development of BOP for 1kW Fuel Cell System", Toshiba Report 2006.

[12] Sevant, N. E., Bloor, M. I. G., and Wilson, M. J., 2000, "Aerodynamic Design of a Flying Wing Using Response Surface Methodology", J. Aircraft, Vol. 37, pp. 562-569.

장 춘 만

1984년 인하대학교 기계공학과 공학사
1986년 인하대학교 기계공학과 공학석사
2000년 큐슈대학교 기계에너지공학과 공학박사

현재 한국건설기술연구원 환경연구실 연구위원
(E-mail : angcm@kict.re.kr)

이 종 성

2009년 안동대학교 기계공학과 공학사
2011년 안동대학교 기계공학과 공학석사

현재 한국건설기술연구원 환경연구실 석사후연구원
(E-mail : leejs@kict.re.kr)